# RSC Advances

## PAPER

# Unprecedent formation of methylsilylcarbonates from iridium-catalyzed reduction of $CO_2$ with hydrosilanes†

Jefferson Guzmán, Pilar García-Orduña, Fernando J. Lahoz [iD] and Francisco J. Fernández-Alvarez [iD] *

The iridium complex $[Ir(\mu\text{-}CF_3SO_3)(\kappa^2\text{-}NSi^{Me2})_2]_2$ (**3**) ($NSi^{Me2}$ = {4-methylpyridine-2-yloxy}dimethylsilyl) has been prepared by reaction of $[Ir(\mu\text{-}Cl)(\kappa^2\text{-}NSi^{Me2})_2]_2$ (**1**) with two equivalents of $AgCF_3SO_3$. The solid structure of **3** evidenced its dinuclear nature, being a rare example of an iridium species with triflate groups acting as bridges. The **3**-catalyzed reduction of $CO_2$ with $HSiMe(OSiMe_3)_2$ affords a mixture of the corresponding silylformate and methoxysilane together with the silylcarbonate $CH_3OCO_2SiMe(OSiMe_3)_2$ (**4a**). This is the first time that the formation of silylcarbonates has been observed from the catalytic reduction of $CO_2$ with silanes. Analogous behaviour has been observed when $HSiMe_2Ph$ and $HSiMePh_2$ were used as reductants.
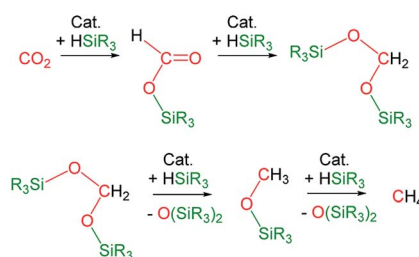
## Introduction

The catalytic reaction of $CO_2$ with silicon-hydrides has proven to be an effective and thermodynamically favoured methodology for its reduction to formate, formaldehyde, methanol or methane (Scheme 1).[1,2]

However, to the best of our knowledge the formation of methylsilylcarbonates, $MeOCO_2SiR_3$ (Fig. 1),[3] as products of the catalytic reduction of $CO_2$ with silicon-hydrides has not been reported so far.

On the other hand, hydrosiloxanes are obtained in large scale as side products of the silicone industry and therefore, the development of catalytic processes effective for the selective reduction of $CO_2$ based on hydrosiloxanes, instead of hydrosilanes, as reductants is of great interest.[4] In this context, in recent years we have focused our research on the application of iridium species as catalysts for the reduction of $CO_2$ with 1,1,1,3,5,5,5-heptamethyltrisiloxane, $HSiMe(OSiMe_3)_2$.[5,6]

Recently, we have described the synthesis and catalytic behavior of the iridium(III) complexes $[Ir(\mu\text{-}Cl)(\kappa^2\text{-}NSi^{Me2})_2]_2$ (**1**) and $[Ir(CF_3CO_2)(\kappa^2\text{-}NSi^{Me2})_2]$ (**2**) ($NSi^{Me2}$ = {4-methylpyridine-2-yloxy}dimethylsilyl) (Scheme 2).[6] Species **2** catalyzed the selective reduction of $CO_2$, depending on the reaction conditions, to silylformate or methoxysilane with $HSiMe(OSiMe_3)_2$.[6] As

a continuation of our studies on the chemistry of iridium complexes with pyridine-2-yloxyI-silyl ligands, we have found that the triflate derivative $[Ir(\mu\text{-}CF_3SO_3)(\kappa^2\text{-}NSi^{Me2})_2]_2$ (**3**) (Scheme 2) catalyzes the reaction of $CO_2$ (3 bar) with $HSiMe(OSiMe_3)_2$ to give a mixture of the corresponding silylformate and methoxysilane along with a new compound that has been characterized by multinuclear NMR spectroscopy as $CH_3OCO_2SiMe(OSiMe_3)_2$ (**4a**). To the best of our knowledge, this is the first time that the formation of silylcarbonates from the catalytic reduction of $CO_2$ with silanes has been observed. The results from these studies are described below.



Scheme 1   Products from the catalytic reduction of $CO_2$ with silicon-hydrides reported so far.



Fig. 1   Methylsilylcarbonates.

*Departamento de Química Inorgánica, Instituto de Síntesis Química y Catálisis Homogénea (ISQCH), Universidad de Zaragoza, Facultad de Ciencias, 50009, Zaragoza, Spain. E-mail: paco@unizar.es*

† Electronic supplementary information (ESI) available: NMR spectra and crystallographic information. CCDC 1972218. For ESI and crystallographic data in CIF or other electronic format see DOI: 10.1039/d0ra00204f
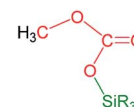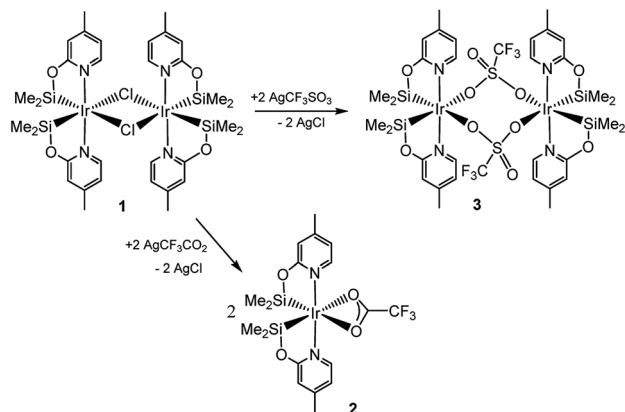
Scheme 2 Preparation of the catalytic precursors **2** and **3**.

## Results and discussion

### Synthesis and characterization of the catalyst precursor

The reaction of complex **1** with two equivalents of $AgCF_3SO_3$ leads to the formation of $[Ir(\mu-CF_3SO_3)(\kappa^2-NSi^{Me2})_2]_2$ (**3**), which has been isolated as a white solid in 89% yield. The solid structure of complex **3** evidenced its dinuclear nature (Fig. 2). As far as we know, **3** is the first example of an iridium species with triflate groups acting as bridges. The molecule exhibits a crystallographic inversion center, with half the molecule as the independent part. Each metal atom shows an octahedral geometry like that found for **1**.[6] Main difference concerns the separation between the iridium atoms (6.0870(2) Å) in **3**, significantly longer than that observed for **1** with chlorine bridges (4.0718(12) Å).
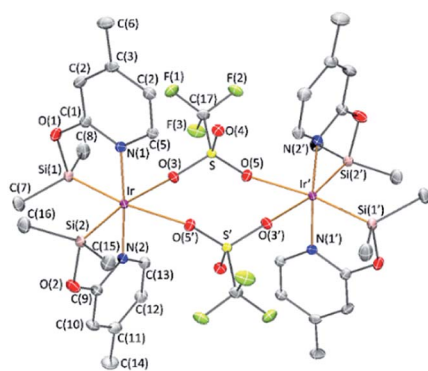


Fig. 2 Molecular structure of compound **3**. For clarity hydrogen atoms have been omitted. Primed atoms are related to unprimed ones through $1 - x$, $1 - y$, $-z$ symmetry operation. Selected bond distances (Å) and angles (°): Ir–Si(1), 2.2570(5); Ir–Si(2), 2.2615(5); Ir–O(3), 2.3653(12); Ir–O(5′), 2.4331(13); Ir–N(1), 2.0590(15); Ir–N(2), 2.0583(15); Si(1)–Ir–Si(2), 91.68(5); Si(1)–Ir–O(3), 95.18(3); Si(1)–Ir–O(5′), 172.22(3); Si(1)–Ir–N(1), 81.57(4); Si(1)–Ir–N(2), 94.94(4); Si(2)–Ir–O(3), 170.27(3); Si(2)–Ir–O(5′), 93.26(3); Si(2)–Ir–N(1), 95.76(4); Si(2)–Ir–N(2), 82.22(4); O(3)–Ir–O(5′), 80.67(4); O(3)–Ir–N(1), 92.06(5); O(3)–Ir–N(2), 90.32(5); O(5′)–Ir–N(1), 91.95(5); O(5′)–Ir–N(2), N(1)–Ir–N(2), 175.94(6).

$^1$H and $^{13}$C{$^1$H} NMR spectra of **3** in $C_6D_6$ show only one pattern of resonances for the four NSi$^{Me2}$ ligands, which agrees with its high symmetry in solution. $^{29}$Si{$^1$H} NMR spectra of **3** show a resonance at $\delta$ 38.2 ppm, corresponding to the four silicon atoms, which compares well to the value of $\delta$ 39.7 ppm reported for **2**.[6] In addition, a singlet resonance at $\delta$ −76.97 ppm in the $^{19}$F{$^1$H} NMR spectra confirm the presence of the triflate ligand.

### 3-Catalyzed reduction of $^{13}CO_2$ with silicon hydrides

Preliminary studies on the **3**-catalyzed reaction of $CO_2$ (3 bar) with $HSiMe(OSiMe_3)_2$ at 298 K showed that 24 hours are required to achieve the conversion of 94% of the starting hydrosiloxane into a mixture of the corresponding silylformate (53.0%) and methoxysilane (21.4%) along with a new compound (25.6%) (TOF = 3.9 h$^{-1}$). This behavior differs from that previously reported for **2**, which under the same reaction conditions catalyzed the full conversion of $HSiMe(OSiMe_3)_2$ into silylformate (93.0%) and methoxysilane (7.0%) in 3.5 h (TOF = 28.6 h$^{-1}$).[6] Therefore, complex **2** is not only more active but also more selective than **3**.

To determine the nature of the new species observed when **3** is used as catalyst for the hydrosilylation of $CO_2$, we decided to study this reaction using isotopically labeled $^{13}CO_2$. Thus, $^1$H and $^{13}$C NMR studies of the **3**-catalyzed (1.0 mol%) reaction of $^{13}CO_2$ (2.7 bar, 323 K, $C_6D_6$) with $HSiMe(OSiMe_3)_2$ were performed. These experiments evidenced, since early reaction stages, the presence of a mixture of $^{13}CH_3O–^{13}CO_2$-$SiMe(OSiMe_3)_2$ (**4a**), together with the corresponding silylformate, $H^{13}CO_2SiMe(OSiMe_3)_2$ (**5a**), and the methoxysilane, $^{13}CH_3OSiMe(OSiMe_3)_2$ (**6a**) (Table 1).

The most characteristic resonance in the $^1$H NMR spectra of **4a** is a doublet of doublets centered at $\delta$ 3.33 ppm ($^1J_{C-H} = 146.9$ Hz; $^3J_{C-H} = 4.1$ Hz) corresponding to the $^{13}CH_3O$ protons

Table 1 Results from **3**-catalyzed reduction of $^{13}CO_2$ (2.7 bar) with $HSiMe(OSiMe_3)_2$ $^a$



| Entry | $T$ (K) | **4a**$^b$ | **5a**$^b$ | **6a**$^b$ | Conversion$^c$ | Time (h) |
|---|---|---|---|---|---|---|
| 1 | 323 | 26.7 | 65.2 | 8.1 | 70 | 3 |
| 2 | 323 | 18.8 | 70.0 | 11.2 | 98 | 12 |
| 3 | 323 | 19.0 | 70.0 | 11.0 | 98 | 24 |
| 4 | 358 | 11.7 | 68.7 | 19.6 | 100 | 24$^d$ |
| 5 | 358 | 8.5 | 68.0 | 23.5 | 100 | 48$^d$ |
| 6$^e$ | 323 | 0 | 0 | 0 | 0 | 24 |

$^a$ General conditions: **3** (1.0 mol%) in 0.5 mL of dry $C_6D_6$. $^b$ Calculated by $^1$H NMR and expressed in mol%. $^c$ Calculated by $^1$H NMR relative to the starting hydrosiloxane and expressed in mol%. $^d$ After 24 h at 323 K. $^e$ Control experiment without iridium catalyst (Fig. S24 see ESI).
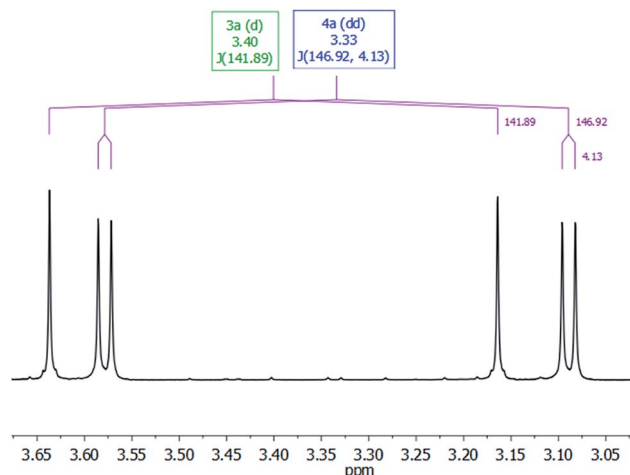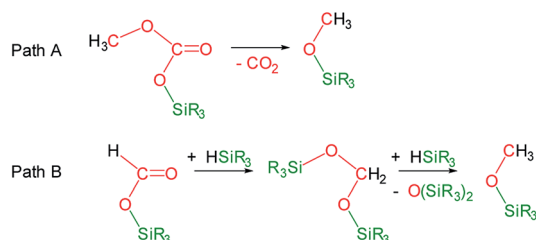
**Fig. 3** $CH_3O$-region of the $^1H$ NMR spectra in $C_6D_6$ of the **3**-catalyzed reaction of $^{13}CO_2$ (2.7 bar) with $HSiMe(OSiMe_3)_2$ at 323 K.

(Fig. 3). This resonance shows a direct C–H bond correlation in the $^1H$–$^{13}C$ HSQC spectra with a doublet resonance centered at $\delta$ 54.1 ppm ($^3J_{C-C} = 1.7$ Hz), assigned to the $^{13}CH_3O$ carbon in the $^{13}C$ APT NMR spectra, and also a C–H bond correlation in the $^1H$–$^{13}C$ HMBC spectra with a doublet resonance that appeared centered at $\delta$ 153.0 ppm ($^3J_{C-C} = 1.8$ Hz), assigned to the $^{13}CO_3$ carbon in the $^{13}C$ APT NMR spectra. These data compare well with those reported for alkyl-silyl-carbonates[3] and support the structure proposed for **4a** in Table 1 (see ESI†).

Under the above described reaction conditions the slow consumption of $HSiMe(OSiMe_3)_2$ was observed (Table 1, entries 1 and 2). Thus, after 12 h the reaction is complete and $^1H$ and $^{13}C\{^1H\}$ NMR spectra evidenced the consumption of all the starting $^{13}CO_2$ and of the 98% of $HSiMe(OSiMe_3)_2$ to give a mixture of **4a** (18.8 mol%), **5a** (70.0 mol%) and **6a** (11.2 mol%) (Table 1, entry 2). Heating this sample for another 12 h at 323 K did not evidence changes in the composition of the mixture (Table 1, entry 3). Interestingly, increasing the temperature at 358 K the slow transformation of **4a** into **6a** occurs (Table 1 entries 4 and 5), in addition, the formation of $^{13}CO_2$ was observed. This outcome agrees with the known thermal behavior of alkyl-silyl-carbonates, $ROCO_2SiR_3$,[3d,e] which thermally decompose to give the corresponding methoxysilane and $CO_2$ (Scheme 3, Path A).

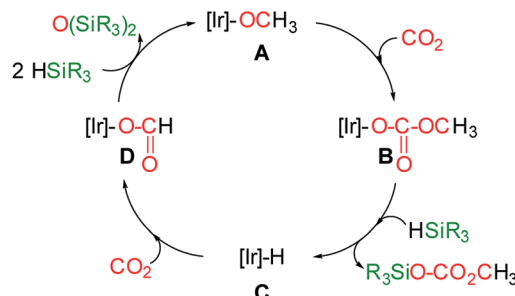The formation of methoxy-silanes from the catalytic reduction of $CO_2$ with hydrosilanes has been so far explained by reaction of bis(silyl)acetals with the corresponding hydrosilane (Scheme 3, Path B).[6,7] Indeed, since it has been observed that at 323 K only traces of **4a** are transformed into **6a** (Table 1 entry 3) it is reasonable to assume that under these conditions **6a** is formed by reactions of the bis(silyl)acetal $^{13}CH_2\{OSiMe(OSiMe_3)_2\}_2$ (**7a**) with $HSiMe(OSiMe_3)_2$. In agreement with this we have observed the presence of traces of **7a** in the NMR spectra of this reaction (ESI†). However, after 24 h of reaction 98% of the starting hydrosiloxane was consumed and therefore, under these conditions, the formation of **6a** at 358 K can only be explained by thermal decomposition of **4a** (Scheme 3, Path B).

Analogous behavior has been observed when $HSiMe_2Ph$ and $HSiMePh_2$ were used as reducing agents. Thus, the formation of the mixtures of methyl-silyl-carbonate $^{13}CH_3O$–$^{13}CO_2SiR_3$ ($SiR_3 = SiMe_2Ph$, **4b**; $SiMePh_2$, **4c**) and the corresponding silylformate and methoxysilane from the **3**-catalyzed reduction of $^{13}CO_2$ with $HSiR_3$ ($SiR_3 = SiMe_2Ph$, $SiMePh_2$) was also observed (ESI†).

It should be mentioned, that the formation of the methyl-silyl-carbonates was not observed along the **2**-catalyzed reduction of $CO_2$ with $HSiMe(OSiMe_3)_2$.[6] In this context, even though species **2** and **3** seem very similar, their reactivity against silanes is very different. Thus, while complex **3** is stable in presence of one equivalent of $HSiMe(OSiMe_3)_2$ at 323 K, the trifluoroacetate ligand in **2** is reduced to give the corresponding silylether $CF_3CH_2OSiR_3$.[5d,6] Therefore, it is reasonable to think that the stability of the triflate ligand could play a role stabilizing reaction intermediates, which could open new paths of reaction, no accessible in **2**-catalyzed $CO_2$ hydrosilylation reactions.

At this point the question arises, how methylsilylcarbonates are formed from the **3**-catalyzed hydrosilylation of $CO_2$. A plausible mechanism proposal is shown in Scheme 4. The formation of methylcarbonates has been explained by insertion of $CO_2$ into the Ir–O bond of iridium–$OCH_3$ species.[8] Therefore, we propose that the reaction of an iridium-methoxy intermediate (**A** in Scheme 4) with $CO_2$ could lead to the methylcarbonate species **B**, which by reaction with $HSiR_3$ would afford the corresponding methylsilylcarbonate and the Ir–H species **C**. The next step, is the reaction of **C** with $CO_2$ to give the iridium–formate intermediate **D**, which according to our previous results has been found to be a thermodynamically favoured



**Scheme 3** Reaction paths for the formation of methoxysilanes from the **3**-catalyzed hydrosilylation of $CO_2$.



**Scheme 4** Plausible mechanism proposal for the formation of methyl-silyl-carbonates from the **3**-catalyzed hydrosilylation of $CO_2$.

process.[5d,6] Finally, the reaction of the iridium–formate **D** with excess of silane could regenerate **A** closing the catalytic cycle.

## Experimental

### General considerations

All manipulations were carried out under an argon atmosphere by Schlenk-type techniques or in a Glovebox MBraun Unilab. Organic solvents were dried by standard procedures and distilled under argon prior to use or obtained oxygen- and water-free from a solvent purification system (Innovative Technologies). $^1H$, $^{13}C$, $^{29}Si$ and $^{19}F$ NMR spectra were obtained on a Bruker AV-300, AV-400 or AV-500 spectrometer. Chemical shifts ($\delta$), reported in ppm, are referenced to the residual solvent peaks and coupling constants ($J$) are reported in Hz.

**Synthesis of 3.** Toluene (10 mL) was added to a light-protected Schlenk containing $[Ir(\mu\text{-}Cl)(\kappa^2\text{-}NSi^{Me2})_2]_2$ (**1**) (300 mg, 0.268 mmol) and silver triflate (151 mg, 0.590 mmol). The mixture was stirred at room temperature for 5 hours and then filtered through Celite. Solvent was removed under reduced pressure and the solid was washed with pentane (3 × 8 mL) to afford a white solid. Yield: 320 mg (89%). $^1H$ NMR (300 MHz, $C_6D_6$, 298 K): $\delta$ 8.73 (d, $J_{H-H}$ = 6.2 Hz, 2H, py), 6.32 (s, 2H, py), 6.02 (d, $J_{H-H}$ = 6.2 Hz, 2H, py), 1.51 (s, 6H, Me-py), 0.72 (s, 6H, Si–Me), 0.41 (s, 6H, Si–Me). $^{13}C$ NMR plus APT and $^1H$–$^{13}C$ HSQC (75 MHz, $C_6D_6$, 298 K): $\delta$ 168.7 (s, py), 152.6 (s, py), 148.7(s, py), 118.4 (s, py), 111.9 (s, py), 20.6 (s, $CH_3$-py), 3.8 (s, $CH_3$–Si), 2.4 (s, $CH_3$–Si). $^{29}Si\{^1H\}$ NMR plus $^1H$–$^{29}Si$ HMBC (60 MHz, $C_6D_6$, 298 K): $\delta$ 38.2 (Ir–Si). $^{19}F$ NMR (282 MHz, $C_6D_6$, 298 K): $\delta$ −76.97 (s, $CF_3SO_3$). High resolution mass spectrometry (ESI$^+$): calc. $m/z$ = 525.1006; found $m/z$ = 525.1004 (M$^+$–$CF_3SO_3$).

**3-Catalyzed (1.0 mol%) reaction of $^{13}CO_2$ with HSiR$_3$.** A Young cap NMR tube was charged with **3** (2.83 mg, 0.0021 mmol), 0.42 mmol of the corresponding silane (114 μL, HSiMe(OSiMe$_3$)$_2$; 64.4 μL, HSiMe$_2$Ph; 83.7 μL, HSiMePh$_2$) and 0.5 mL of $C_6D_6$. Argon gas was evacuated by three freeze-pump-thaw cycles. Then the tube was pressurized with $^{13}CO_2$ (2.7 bar), heated at 323 K and monitored by NMR spectroscopy.

**Selected data for 4a.** $^1H$ NMR plus HSQC $^1H$–$^{13}C$ (300 MHz, $C_6D_6$, 298 K): $\delta$ 3.33 (dd, $^1J_{H-C}$ = 146.9 Hz, $^3J_{H-C}$ = 4.1 Hz, 3H, $CH_3OCO_2$). $^{13}C\{^1H\}$ plus HSQC and HMBC $^1H$–$^{13}C$ (75 MHz, $C_6D_6$, 298 K): $\delta$ 153.0 (d, $^2J_{C-C}$ = 1.7 Hz, $CO_3$), 54.1 (d, $^2J_{C-C}$ = 1.7 Hz, $CH_3O$). Selected data for **4b**: $^1H$ NMR plus HSQC $^1H$–$^{13}C$ (300 MHz, $C_6D_6$, 298 K): $\delta$ 3.30 (dd, $^1J_{H-C}$ = 147.1 Hz, $^3J_{H-C}$ = 4.1 Hz, 3H, $CH_3OCO_2$). $^{13}C\{^1H\}$ plus HSQC and HMBC $^1H$–$^{13}C$ (75 MHz, $C_6D_6$, 298 K): $\delta$ 154.1 (d, $^2J_{C-C}$ = 1.7 Hz, $CO_3$), 54.2 (d, $^2J_{C-C}$ = 1.7 Hz, $CH_3O$). Selected data for **4c**: $^1H$ NMR plus HSQC $^1H$–$^{13}C$ (300 MHz, $C_6D_6$, 298 K): $\delta$ 3.23 (dd, $^1J_{H-C}$ = 147.1 Hz, $^3J_{H-C}$ = 4.1 Hz, 3H, $CH_3OCO_2$). $^{13}C\{^1H\}$ plus HSQC and HMBC $^1H$–$^{13}C$ (75 MHz, $C_6D_6$, 298 K): $\delta$ 153.9 (d, $^2J_{C-C}$ = 1.8 Hz, $CO_3$), 54.3 (d, $^2J_{C-C}$ = 1.8 Hz, $CH_3O$).

**Crystal structure determination of complex 3.** Single crystal X-ray diffraction data were collected at 100(2) K with graphite-monochromated Mo Kα radiation ($\lambda$ = 0.71072 Å) using narrow frame rotation ($\Delta\omega$ = 0.3°) on a Bruker Smart APEX diffractometer. Measured intensities were integrated and corrected for absorption effects with SAINT+[9] and SADABS[10]

programs, included in APEX2 package. The structure was solved with direct methods with SHELXS-2013 (ref. 11) and refined by full-matrix least-squares refinement on $F^2$ with SHELXL-2018 (ref. 12) program, included in WingX package.[13] The disordered solvent region has been analyzed with SQUEEZE program.[14]

CCDC 1972218 contains the supplementary crystallographic data for this paper.

Crystal data compound **3.** $C_{34}H_{48}F_6Ir_2N_4O_{10}S_2Si_4\cdot0.5(H_2O)$; $M$ = 1364.65; colourless prism 0.140 × 0.240 × 0.330 mm$^3$; triclinic $P\bar{1}$, $a$ = 9.0468(5), $b$ = 12.0453(6), $c$ = 12.0619(7) Å, $\alpha$ = 66.4720(10), $\beta$ = 88.5460(10), $\gamma$ = 88.7690(10)°, $V$ = 1204.65(11) Å$^3$; $Z$ = 1; $D_c$ = 1.881 g cm$^{-3}$; $\mu$ = 5.783 mm$^{-1}$; $T_{min}/T_{max}$: 0.1676/0.5996; 23 425/5849 reflections measured/unique ($R_{int}$ = 0.0179), number of data/restraint/parameters 5849/0/286, $R_1(F^2)$ = 0.0131 (5771 reflections, $I > 2\sigma(I)$) and w$R(F^2)$ = 0.0324 (all data), final GoF = 1.034, largest difference peak: 0.988 e Å$^{-3}$.

## Conclusions

In conclusion, the use of triflate, instead of trifluoroacetate, as ancillary ligand in the chemistry of Ir-(NSi$^{Me2}$)$_2$ species allows the preparation of **3**, which is a rare example of a dinuclear iridium complex with triflate ligands acting as bridges.

$^1H$ NMR studies of the **3**-catalyzed reduction of $CO_2$ with hydrosilanes evidenced the unprecedent formation of methylsilylcarbonates as reaction products, together with the corresponding silylformate and methoxysilane.

The results of this investigation show that the formation of methoxysilanes during the catalytic reduction of $CO_2$ with silanes, which traditionally has been explained by the catalytic reaction of bis(silyl)acetals with silanes, could also be consequence of thermal decomposition of the corresponding methylsilylcarbonate.

## Conflicts of interest

There are no conflicts to declare.

## Acknowledgements

## Notes and references

1 (a) J. Chen, M. McGraw and E. Y.-X. Chen, *ChemSusChem*, 2019, **12**, 4543–4569; (b) F. J. Fernández-Alvarez and L. A. Oro, *ChemCatChem*, 2018, **10**, 4783–4796; (c) C. Chauvier and T. Cantat, *ACS Catal.*, 2017, 7, 2107–2115; (d) F. J. Fernández-Alvarez, A. M. Aitani and L. A. Oro, *Catal. Sci. Technol.*, 2014, **4**, 611–624.

2 For examples of transition-metal free catalyzed processes see: K. Motokura, C. Nakagawa, R. A. Pramudita and

Y. Manaka, *ACS Sustainable Chem. Eng.*, 2019, **7**, 11056–11061; and references therein.

3 (*a*) Y. Yamamoto and D. S. Tarbell, *J. Org. Chem.*, 1971, **36**, 2954–2956; (*b*) M. Paul, J. Dunoguès, R. Calas and E. Frainnet, *J. Organomet. Chem.*, 1972, **38**, 267–274; (*c*) Y. Yamamoto, D. S. Tarbell, J. R. Fehlner and B. M. Pope, *J. Org. Chem.*, 1973, **38**, 2521–2525; (*d*) R. Tacke, M. Link, A. Bentlage-Felten and H. Zilch, *Z. Naturforsch.*, 1985, **40b**, 942–947; (*e*) H. Yildirimyan and G. Gattow, *Z. Anorg. Allg. Chem.*, 1985, **521**, 135–144.

4 D. Addis, S. Das, K. Junge and M. Beller, *Angew. Chem., Int. Ed.*, 2011, **50**, 6004–6011.

5 (*a*) R. Lalrempuia, M. Iglesias, V. Polo, P. J. Sanz Miguel, F. J. Fernández-Alvarez, J. J. Pérez-Torrente and L. A. Oro, *Angew. Chem., Int. Ed.*, 2012, **51**, 12824–12827; (*b*) E. A. Jaseer, M. N. Akhtar, M. Osman, A. Al-Shammari, H. B. Oladipo, K. Garcés, F. J. Fernández-Alvarez, S. Al-Khattaf and L. A. Oro, *Catal. Sci. Technol.*, 2015, **5**, 274–279; (*c*) A. Julián, E. A. Jaseer, K. Garcés, F. J. Fernández-Alvarez, P. García-Orduña, F. J. Lahoz and L. A. Oro, *Catal. Sci. Technol.*, 2016, **6**, 4410–4417; (*d*) A. Julián, J. Guzmán, E. A. Jaseer, F. J. Fernández-Alvarez, R. Royo, V. Polo, P. García-Orduña, F. J. Lahoz and L. A. Oro, *Chem.–Eur. J.*, 2017, **23**, 11898–11907; (*e*) A. I. Ojeda-Amador, J. Munarriz, P. Alamán-Valtierra, V. Polo, R. Puerta-Oteo, M. V. Jiménez, F. J. Fernández-Alvarez and J. J. Pérez-Torrente, *ChemCatChem*, 2019, **11**, 5524–5535.

6 J. Guzmán, P. García-Orduña, V. Polo, F. J. Lahoz, L. A. Oro and F. J. Fernández-Alvarez, *Catal. Sci. Technol.*, 2019, **9**, 2858–2867.

7 (*a*) T. C. Eisenschmid and R. Eisenberg, *Organometallics*, 1989, **8**, 1822–1824; (*b*) S. N. Riduan, Y. Zhang and J. Y. Ying, *Angew. Chem., Int. Ed.*, 2009, **48**, 3322–3325; (*c*) S. N. Riduan, J. Y. Ying and Y. Zhang, *ChemCatChem*, 2013, **5**, 1490–1496; (*d*) D. S. Morris, C. Weetman, J. T. C. Wennmacher, M. Cokoja, M. Drees, F. E. Kühn and J. B. Love, *Catal. Sci. Technol.*, 2017, **7**, 2838–2845; (*e*) D. Specklin, F. Hild, C. Fliedel, C. Gourlaouen, L. F. Veiros and S. Dagorne, *Chem.–Eur. J.*, 2017, **23**, 15908–15912; (*f*) M. Saleh, D. R. Powell and R. J. Wehmschulte, *Organometallics*, 2017, **36**, 4810–4815.

8 N. Hazari and J. E. Heimann, *Inorg. Chem.*, 2017, **56**, 13655–13678.

9 *SAINT+, version 6.01: Area-Detector Integration Software*, Bruker AXS, Madison, 2001.

10 (*a*) *SADABS (Version 2016/02)*, Bruker AXSMadison; (*b*) L. Krause, R. Herbst-Irmer, G. M. Sheldrick and D. Stalke, *J. Appl. Crystallogr.*, 2015, **48**, 3–10.

11 (*a*) G. M. Sheldrick, *Acta Crystallogr., Sect. A: Found. Crystallogr.*, 1990, **46**, 467–473; (*b*) G. M. Sheldrick, *Acta Crystallogr., Sect. A: Found. Crystallogr.*, 2008, **64**, 112–122.

12 G. M. Sheldrick, *Acta Crystallogr., Sect. C: Struct. Chem.*, 2015, **71**, 3–8.

13 L. J. Farrugia, *J. Appl. Crystallogr.*, 2012, **45**, 849–854.

14 P. van der Sluis and A. L. Spek, *Acta Crystallogr., Sect. A: Found. Crystallogr.*, 1990, **46**, 194–201.